ELSEVIER

Polymer 42 (2001) 261–272

polymer

www.elsevier.nl/locate/polymer

The effect of processing variables on the morphology of electrospun nanofibers and textiles

J.M. Deitzel, J. Kleinmeyer, D. Harris, N.C. Beck Tan*

US Army Research Laboratory, Polymers Research Branch, Materials Division Bldg. 4600, Deer Creek Loop, Attn: AMSRL-WM-MA, Aberdeen Proving Grounds, Aberdeen, MD 21005-5069, USA

Received 20 December 1999; received in revised form 17 March 2000; accepted 20 March 2000

Abstract

Electrospinning is a process that produces continuous polymer fibers with diameters in the sub-micron range through the action of an external electric field imposed on a polymer solution or melt. Non-woven textiles composed of electrospun fibers have a large specific surface area and small pore size compared to commercial textiles, making them excellent candidates for use in filtration and membrane applications. While the process of electrospinning has been known for over half a century, current understanding of the process and those parameters, which influence the properties of the fibers produced from it, is very limited. In this work, we have evaluated systematically the effects of two of the most important processing parameters: spinning voltage and solution concentration, on the morphology of the fibers formed. We find that spinning voltage is strongly correlated with the formation of bead defects in the fibers, and that current measurements may be used to signal the onset of the processing voltage at which the bead defect density increases substantially. Solution concentration has been found to most strongly affect fiber size, with fiber diameter increasing with increasing solution concentration according to a power law relationship. In addition, electrospinning from solutions of high concentration has been found to produce a bimodal distribution of fiber sizes, reminiscent of distributions observed in the similar droplet generation process of electrospray. In addition, we find evidence that electrostatic effects influence the macroscale morphology of electrospun textiles, and may result in the formation of heterogeneous or three-dimensional structures.

Keywords: Electrospinning; Nanofiber; Morphology

1. Introduction

Polymer fibers are used in a wide variety of applications ranging from textiles to composite reinforcement. Traditional methods of obtaining polymer fibers include melt spinning [1], spinning from solution or liquid crystalline state, and forming fibers from a gel state [2]. Typical fiber diameters produced by these methods range from 5 to 500 nm, with the lower limit of fiber diameter that is consistently achievable on the order of magnitude of a micron. Recently [3], there has been increased interest in another method of fiber production, electrospinning, which can consistently produce fibers that are sub-micron in diameter. Textiles produced from these fibers are showing promise for exploitation in clothing and filtration applications [3,4]. In addition, there is some evidence [5] indicating that electrospun fibers have a sizable static charge making it possible to manipulate them into three-dimensional (3) structures during their deposition. This property, together with the small pore size and high surface area inherent in electrospun nanofiber non-woven fabrics [3–5], has implications for the use of electrospun fibers in biomedical applications such as scaffoldings for tissue growth [6].

The electrospinning process can be considered a variation of the better-known electrospray process. It has been understood for most of this century that it is possible to use electrostatic fields to form and accelerate liquid jets from the tip of a capillary [7–9]. The surface of a hemispherical liquid drop suspended in equilibrium at the end of a capillary will be distorted into a conical shape in the presence of an electric field. A balancing of the repulsive force resulting from the induced charge distribution on the surface of the drop with the surface tension of the liquid causes this distortion. Once a critical voltage, V_c, is exceeded a stable jet of liquid is ejected from the cone tip. The jet breaks up into droplets as a result of surface tension in the case of low viscosity liquids. For high viscosity liquids the jet does not break up, but travels as a jet to the grounded target [8]. The first case is known as electrospraying and is used in many industries to

* Corresponding author. Tel.: + 1-410-306-700; fax: + 1-410-306-676.
E-mail address: nora@arl.nil (N.C. Beck Tan).

0032-3861/01/$ - see front matter
PII: S0032-3861(00)00250-0

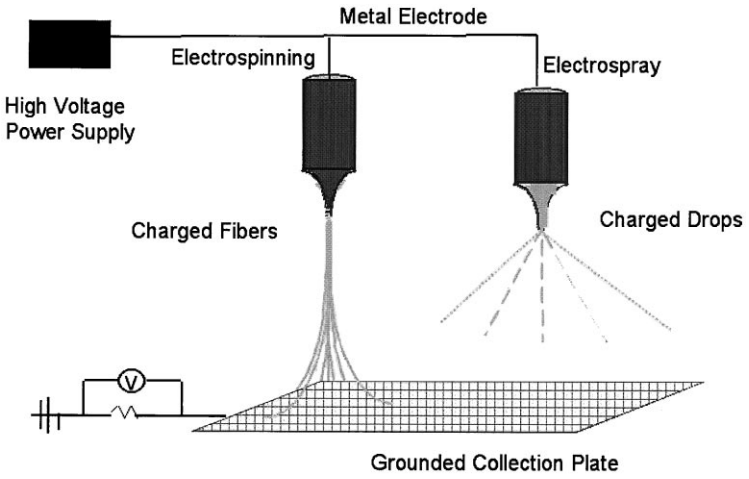

Fig. 1. Schematic diagram of the electrospinning and electrospray processes.

obtain aerosols composed of sub-micron drops with narrow distributions. When applied to polymer solutions and melts, the second case is known as electrospinning and it generates polymer fibers that are sub-micron in diameter.

As a result of both commercial and scientific interest in electrospray, much effort has been made to understand and control the process [10–12]. Taylor established that the equilibrium shape of a hemispherical drop changes to a cone shape in an electric field. When the voltage applied to the drop exceeds a critical value, a liquid jet will initiate at the vertex of the cone. After jet initiation, the cone shape cannot be maintained if the flow of solution to the capillary tip does not match the rate at which solution is being removed by the jet [8,9]. However, the electrostatically driven jet may continue to flow after the collapse of the cone, even though the shape of the surface from which the established jet originates, to be referred to as originating surface here after, is radically different from the conical shape seen at the time of jet initiation. The impact of the shape of originating surface and other processing variables (solution viscosity, accelerating voltage) on the size and size distribution of electrosprayed droplets are discussed in review articles by Cloupeau and Prunet-Foch [10] and Grace and Marijnissen [11]. The major emphasis in these two articles is the identification of different modes of electrospray. These modes are characterized by varying degrees of instability associated with the shape of the originating surface, and are achieved by manipulating the flow rate of solution to the capillary tip and the applied voltage. The electrospray modes affect the average droplet size and droplet size distribution, with the Taylor-cone mode

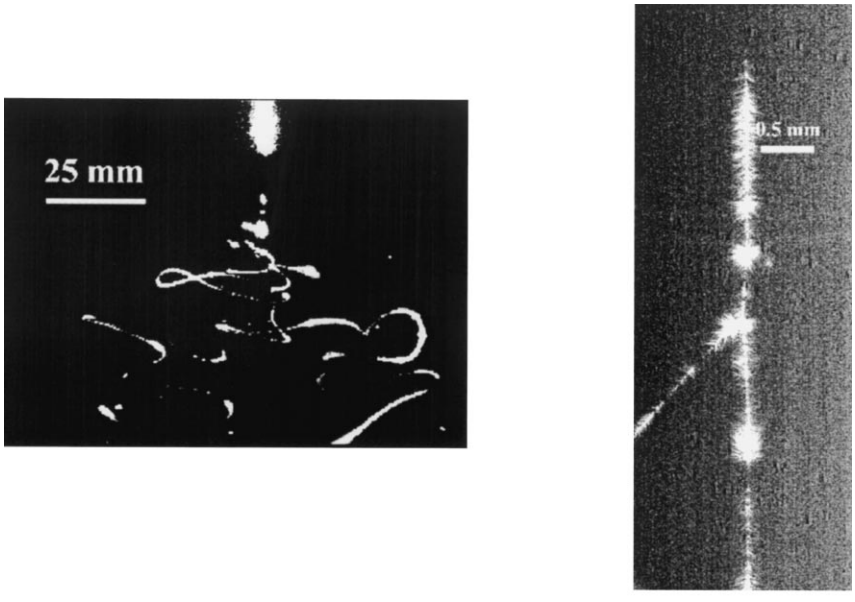

Fig. 2. High speed images of the electrospinning process: (a) a single jet being spun from a 6 wt% solution of PEO in water; and (b) A splaying event captured during the electrospinning of a fiber from a 10 wt% PEO/water solution.

producing the smallest average droplet sizes and narrowest droplet size distribution [10–12]. These results are of interest because processing parameters influencing droplet size and size distribution in the electrospray process may similarly influence the morphology of polymer fibers formed using the electrospinning process.

If the electrospray process is applied to a polymer solution of sufficient viscosity (~1–200 poise), the initial jet does not break up into individual drops (Fig. 1). Instead, the solvent will evaporate as the jet proceeds to the target, leaving behind polymer fiber. The jet often follows a bending and turning trajectory as it travels to the target, and under certain conditions may also split or splay into smaller fibers [5,13–18]. The small diameters of electrospun fibers are achieved as a result of a single filament undergoing drawing and splaying analogous to the droplet disintegration described for electrospray [18].

Interest in the electrospinning process has increased in recent years [13–17]. Most of the literature on electrospinning has explored the types of polymer solvent systems from which fibers can be produced. A few studies have also addressed the processing/property relationships in electrospun polymer fibers, either directly or indirectly. Processing parameters considered have included solution concentration and viscosity effects, spinning atmosphere effects, accelerating voltage effects and tip-to-target distance. Solution viscosity has been found to influence fiber diameter [5,15–17], initiating droplet shape [5,16], and the jet trajectory [5,16,18,19]. Increasing solution viscosity has been associated with the production of larger diameter fibers [5–17]. Baumgarten [16] has also correlated spinning atmosphere with the occurrence of the jet splaying phenomena. Though splaying effects have been observed recently by Reneker, et. al. [13–15,18], and commonly in our laboratory under certain experimental conditions (Fig. 2), they have not been reported by all investigators [19–21]. Other processing variables, such as acceleration voltage, electrospinning current and tip-to-target distance have not been investigated fully, but have been linked with fiber morphology and defect structures [5,15–17,22,23].

It is clear from the background literature for both the electrospray and electrospinning processes that the structure and morphology of the final product, be it particles or fibers, are determined by a synergetic effect of solution parameters and electrostatic forces. These parameters include viscosity, surface tension, concentration, and dielectric properties of the spinning solution or melt, and process parameters such as the feed rate of the solution to the tip, and the acceleration voltage. Work that addresses the effect of the variables mentioned above on the sub-micron fiber structure and morphology is in its early stages. The purpose of the current work is to look systematically at the effects of accelerating voltage and solution concentration on the structure and morphology of electrospun polyethylene oxide fibers. We find that significant changes in fiber diameter, size distribution, and morphology accompany changes in these variables. Analogies are drawn to similar experiments found in the electrospray literature.

2. Experimental

The solutions used in the electrospinning experiments were prepared using 400,000 molecular weight Poly(ethylene oxide) (PEO) purchased from Scientific Polymer Products. This material was dissolved in HPLC grade water to make solutions with concentrations ranging from 4 to 10 wt%. Surface tensions for each solution were determined by the Wilhelmy Balance method using glass microscope cover slides that were cleaned with a butane torch. Solution viscosities were measured with a TA Instruments AR 1000-N constant stress rheometer in a cone and plate geometry. Each experiment was performed at 20°C with a 4 cm and 2° cone. Solutions were spun from a 50 ml syringe with a 23 gauge (diameter = 0.35 mm) needle. A Gamma High Voltage Research ES30P power supply was used to produce voltages ranging from 5.5–15.0 kV. Various electrically grounded materials, such as aluminum screen, were used as targets.

The experimental set up for the study of the effect of concentration on electrospun fiber morphology was as follows. A 20–30 ml quantity of a PEO/water solution was placed in a 50 ml syringe. The syringe was then clamped to a ringstand that was 6.5 in. above a grounded metal screen. The power supply was connected to the metal syringe tip. Constant pressure in the form of a weight was applied to the syringe so that a small, stable drop of solution was suspended above the target. The weight applied to the syringe plunger was increased with increasing solution concentration to achieve similar initial conditions. Once this stable initial condition was achieved, a voltage of 7.0 kV was applied to the syringe tip to initiate the jet. Typical time to collect the samples, in the form of non-woven fiber mats was about 24 h. The electrospun fiber mats were held under vacuum at ambient temperature for 24 h in order to ensure complete drying of the sample.

The physical setup for the study of the effect of voltage on nanofiber morphology was the same as that for the concentration study. A quantity of 7 wt% PEO/water solution was placed in the syringe and the electrospinning process was carried out for a number of voltages. The weight applied to the syringe plunger was held constant.

Morphological observations were made with a Phillips Electroscan Environmental Scanning Electron Microscopy (ESEM). The samples were held at a temperature of 4°C using a Peltier stage during the experiment to minimize melting of the fibers by heat generated from the electron beam.

Optical micrographs were taken with a Photometrics cooled CCD camera with a 3k by 2k chip. The camera was attached to a Questar Schmidt-Cassegrain telescope in order to achieve high magnification from a distance.

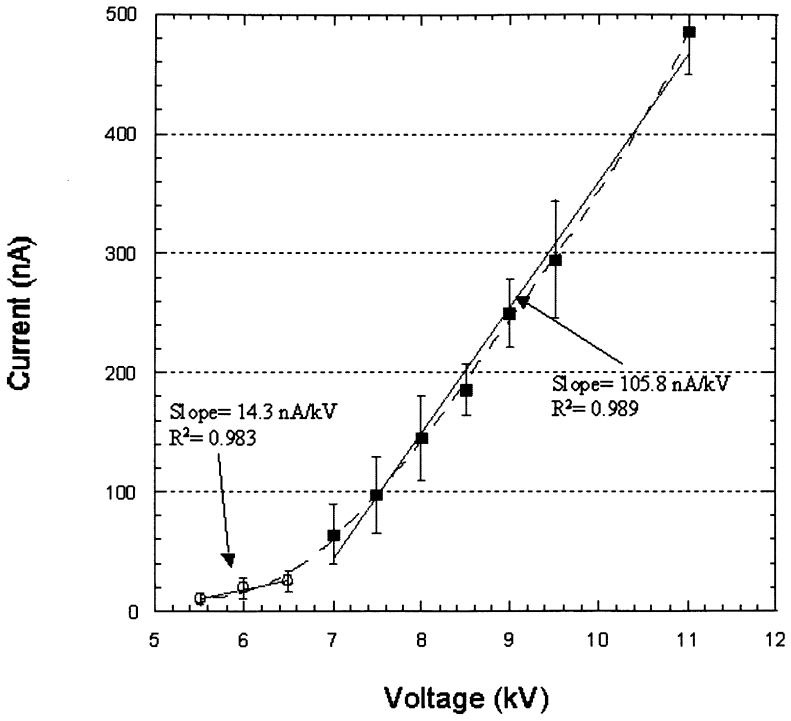

Fig. 3. Electrospinning current measured as a function of spinning voltage.

3. Results and discussion

3.1. Nanofiber morphology: voltage dependence

As has been discussed in the introduction, the electrospray process can be sustained in a variety of modes characterized by the shape of the surface from which the liquid jet originates. These modes occur at different voltages and have significant effects on droplet size distribution and current transport. Although distinct modes might be difficult to isolate and observe in the electrospinning process, it is expected that the degree of instability of the liquid surface from which the jet originates should produce changes in the electrospun fiber morphology. It has been verified experimentally that the shape of the initiating drop changes with spinning conditions (voltage, viscosity, feed rate) [16].

In electrospinning experiments, the electric current associated with the process can be measured with a microampmeter. The droplets or fibers transport charge across the gap between the charged needle and the electrically grounded target, closing the circuit. For electrospray, an increase in frequency of drop formation and a corresponding change in the measured electrospray current [12] accompany a change in the mode of spray initiation. As the electrospray voltage is increased smoothly, the measured current undergoes stepwise increases that correspond to the observed changes in jet initiation modes. In the case of electrospinning, the electric current due to the ionic conduction of charge in the polymer solution is usually assumed small enough to be negligible [16]. The only mechanism of charge transport is the flow of polymer from the tip to the target. Thus, an increase in the electrospinning current generally reflects an increase in the mass flow rate from the capillary tip to the grounded target when all other variables (conductivity, dielectric constant, and flow rate of solution to the capillary tip) are held constant. For the PEO/water system, the spinning current has been found to increase with increasing voltage (Fig. 3). This observation is in qualitative agreement with results reported Jaeger et al. [22]. Initiation of the jet occurs at a voltage of 5.5 kV. The electrospinning current increases slowly with increasing voltage in the range of 5.5–7 kV. The slope of the curve increases sharply above 7 kV, in a manner similar to a second-order transition. This behavior is quite different than the sharp step increases observed in electrospray systems that have been associated with changes in mode [12].

While there are no step increase in the electrospinning current that would signal a change in mode, a change in electrospun fiber morphology may be correlated to the observed change in the slope of the electrospinning current as a function of voltage (Figs. 4–6). The morphology of the electrospun PEO nanofibers changes from that of primarily straight, defect-free fibers spun at an initiating voltage of 5.5 kV, to one in which the fiber mats contain a high density of beads when spun at an initiating voltage of 9.0 kV. For the PEO/water system studied here, this bead structure becomes prevalent at a voltage of about 7 kV, coincident with the change in slope in the plot of electrospinning current versus voltage (Fig. 3). This coincidence suggests that by monitoring the spinning current, one may be able to control the bead defect density in the electrospun fibers.

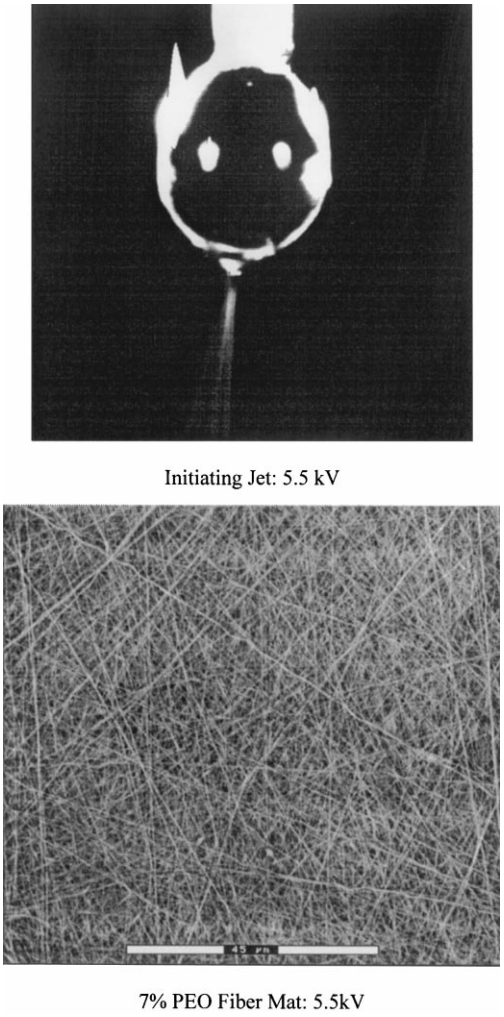

Fig. 4. Initiating jet (top) and the corresponding fibers (bottom) produced by spinning of a 7 wt% PEO/water solution at a voltage of 5.5 kV.

The change in fiber morphology with voltage also correlates to changes in the originating droplet shape. At low voltages (Fig. 4), a droplet of solution remains suspended at the end of the syringe needle, and the fiber jet originates from a cone at the bottom of the droplet. The cone has a semi-vertical angle of about 50°, in agreement with Taylor's theoretical prediction of 49.3° for a viscous fluid in an electric field [8,9]. The shape of this surface from which the polymer jet originates is similar in appearance to the microdripping jet mode eported in literature [12], where the jet originates from the bottom of a drop whose diameter is larger than the capillary diameter. The nanofibers produced under these conditions have a cylindrical morphology with few bead defects present. As voltage is increased, the volume of the droplet decreases. At voltages of 7 kV or more, the cone has receded and the jet originates from the liquid surface within the syringe tip (Fig. 5). The electrospun fibers produced still have essentially a cylindrical morphology, but there is a distinct increase in number of bead defects present in the fiber mat. At 9.0 kV the solution jet appears to be initiating directly from the tip with no externally visible droplet or cone (Fig. 6). At this voltage, the jet moves around the edge of the syringe tip, indicating that the jet originates on the inside surface of the syringe needle, where the edge of the liquid surface meets the needle wall. The fibers produced under these conditions have a high density of bead defects. In fact, the bead defect density increases very sharply with voltage about 7 kV above (Fig. 7).

The formation of bead defects in electrospun fibers has been described in several papers [17,21–23], and bead formation has been initiated by varying solution surface tension [17] and solution charge density, and by charge neutralization [17]. In this experiment only the electrospinning voltage was varied while the solution properties were kept constant. The possibility that some small fluctuation in the charge density occurred as a result of charge dissipation from the tip into the atmosphere cannot be dismissed entirely. However, no overt evidence (sparks, snaps, or corona) of corona discharge were observed at voltages below 13 kV.

From the results discussed in the preceding paragraphs, it is seen that electrospinning does not exhibit numerous discrete modes like those observed in electrospray experiments. However, it has been demonstrated that above a critical voltage there are significant changes in the shape of the originating surface and the voltage dependence of the electrospinning current, and that these changes correspond to an increase in the number of bead defects observed in the electrospun fiber mats. To the best of our knowledge, the results presented here are the first to correlate the bead morphology with the shape of the liquid surface from which the jet originates. The change in the shape of the liquid surface reflects a change in the mass balance that occurs at the end of the capillary tip. Increasing the voltage causes the rate at which solution is removed from the capillary tip to exceed the rate of delivery of solution to the tip needed to maintain the conical shape of the surface. This shift in the mass balance results in a sustained but increasingly less stable jet, as evidenced by the precession of the jet observed at 9 kV. Our results suggest that fiber bead density increases with the increasing instability of the jet at the spinning tip, and may be minimized through control of material flow rates to and from the tip.

3.2. Nanofiber morphology: concentration dependence

It has been shown in the electrospray literature that solution concentration has a significant effect on the final size and distribution of particles [12]. Solution surface tension and viscosity also play important roles in determining the range of concentrations from which continuous fibers can be obtained in electrospinning. At low viscosities ($\eta < 1$ poise), surface tension is the dominant influence on fiber morphology and below a certain concentration drops will form instead of fibers. At high concentrations ($\eta > 20$ poise), processing will be prohibited by an inability to control and maintain the flow of a polymer solution to the tip of the needle and by the cohesive nature of the high viscosity

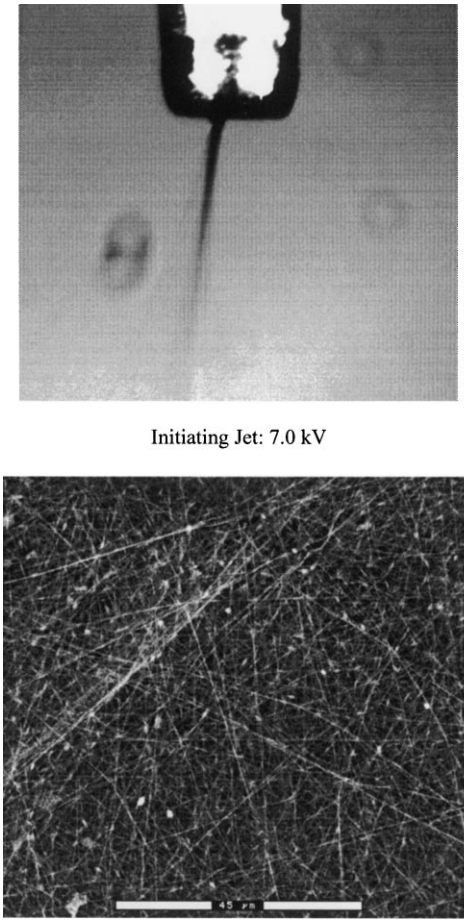

Fig. 5. Initiating jet (top) and the corresponding fibers (bottom) produced by spinning of a 7 wt% PEO/water solution at a voltage of 7.0 kV.

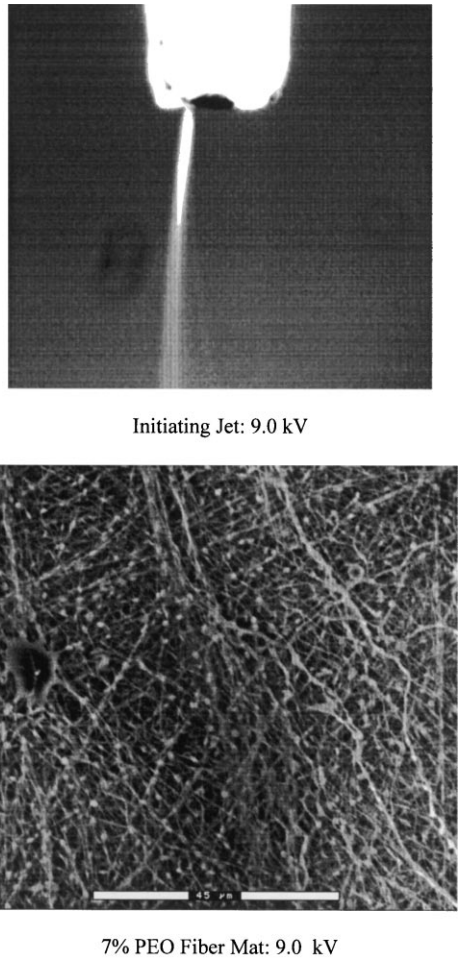

Fig. 6. Initiating jet (top) and the corresponding fibers (bottom) produced by spinning of a 7 wt% PEO/water solution at a voltage of 9.0 kV.

solutions. In this study of spinning from aqueous solutions of 400,000 molecular weight PEO, concentrations in the range of 4–10 wt% produced fibers. These solutions had viscosities in the range of 1–20 poise and surface tensions in the range of 55–35 dynes/cm (Fig. 8). At concentrations below 4 wt%, the electrospinning process generated a mixture of fibers and droplets. Electrospinning from solutions with concentrations higher than 10 wt% was prohibited by their high viscosity. The higher viscosity solutions proved extremely difficult to force through the syringe needle of the apparatus used in these experiments, making the control of the solution flow rate to the tip unstable. For solutions with concentration of 15 wt% or more, the droplet at the end of the capillary stretched into a thick (diameter ~ 0.5 mm) strand that oscillated in the electric field. Eventually the strand gained enough mass that gravity caused it to separate from the capillary and land on the ground plane. At no time was a sustainable jet achieved. Although the range of concentrations that produce fibers will obviously vary depending on the polymer/solvent system used, the forces of viscosity and surface tension will determine the upper and lower boundaries of processing window, if all other variables are held constant.

Even within the fiber processing window, varying solution concentration alters the morphology of the nanofibers formed. Electron micrographs of fibers electrospun from 4 and 10 wt% concentrations of PEO/water solutions are shown in Fig. 9. These images demonstrate the two extremes in the fiber morphologies observed as a result of varying solution concentration within the processable range. At the low concentration end of the processing window, the fibers have an irregular, undulating morphology with large variations in diameter along a single fiber. There are numerous junctions and bundles of fibers. At the high concentration end of the processing window, the nanofibers have a regular, cylindrical morphology and on average have a larger and more uniform diameter. The presence of fiber junctions and bundles of fibers in the non-woven fiber mat electrospun from the 4 wt% PEO solution is evidence that the polymer fibers are still wet when they hit the collection screen. At higher concentrations, the fibers exhibit a straight, cylindrical morphology with relatively few fiber bundles and junctions indicating that the fibers are mostly dry when they reach the collection screen. The apparent change in morphology may be reflective of the lower

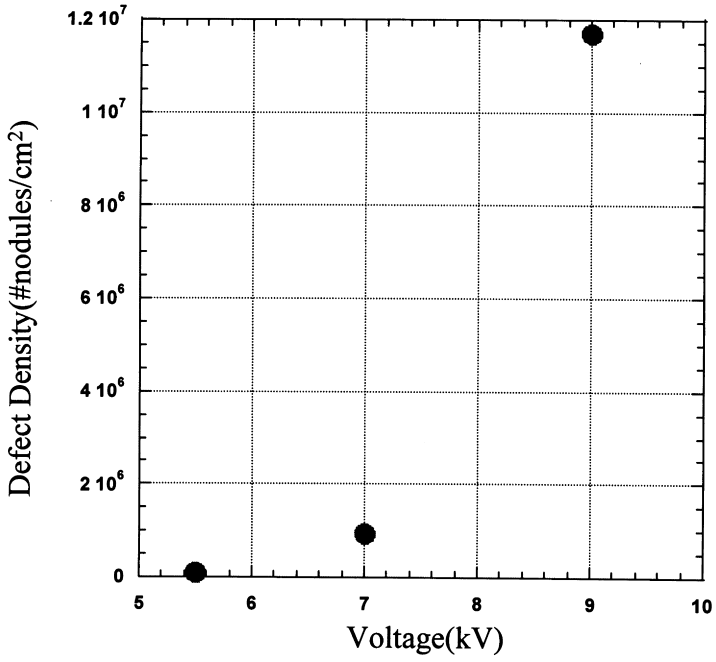

Fig. 7. Area density of bead defects in electrospun fiber textiles as a function of the electrospinning voltage under which they were produced.

surface tension and solvent content in the high concentration solutions. In addition, measured mass deposition rates were found to decrease as the solution concentration increased, from about 5 to about 2 mg/h. The effect of concentration on the average diameter of electrospun nanofibers is quantified in Figs. 10 and 11. Two basic observations can be made: first, the average diameter of electrospun PEO fibers increases with spinning solution concentration; and second, the fiber population exhibits a bimodal size distribution at concentrations of above 7 wt% PEO/water. In this system, the average diameter of the electrospun fibers is related to the solution concentration through a power law relationship with an exponent of about 0.5. The relationship between solution concentration and droplet diameter in electrospray

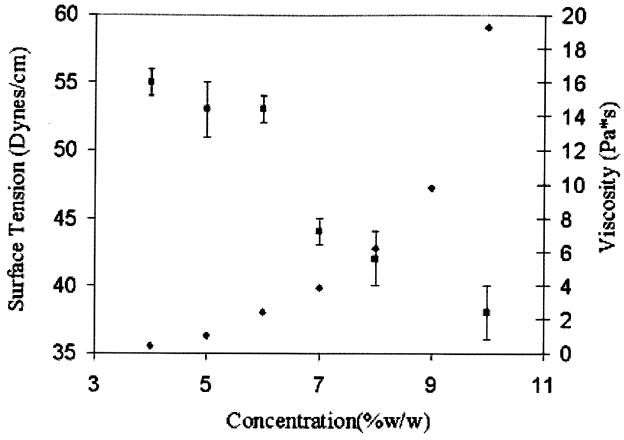

Fig. 8. Dependence of solution surface tension (squares) and solution viscosity (diamonds) as a function of concentration for PEO/water solutions.

also follows a power law relationship, with exponent of 0.3 [12]. Others have observed a power law relationship between fiber diameter and electrospinning solution concentration for electrospun polymer fibers, though the exponents differed [16]. The differences in exponential power dependence may be attributed to the in-flight splitting or splaying of electrospinning jet. Several groups have reported splaying phenomena occurring during fiber production [15]. We have observed this phenomena in our laboratory, and it is prevalent under certain conditions in the spinning of PEO/water solutions. However, other researchers have reported only single fiber production (the absence of splaying) in different polymer/solvent systems when electrospun under ambient conditions [16,18–20]. The presence or absence of the splaying phenomena could result in different power law dependence for different polymer/solvent systems.

One of the most interesting results from our concentration dependence studies on the electrospun PEO/water system is the appearance of a bimodal distribution of fiber diameters in fibers spun from higher concentration solutions. Once the solution concentration reaches about 8 wt%, a second population of smaller fibers is produced, in addition to the primary population. This secondary population of fibers have diameters about one third of those in the primary population and make up a larger fraction of the total number of (Figs. 10 and 12). Though this fiber diameter distribution is reminiscent of the bimodal droplet distribution that has been reported in electrospray literature, this is the first time it has been reported to occur in the electrospinning process. The bimodal distribution observed in electrosprayed droplet populations similarly occurs when higher concentration solutions are sprayed, and is believed to be associated with the formation of satellite

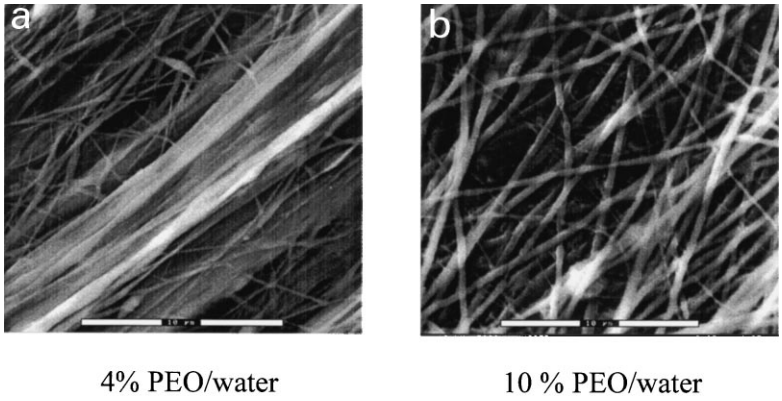

Fig. 9. Scanning electron micrographs of nanofibers electrospun from: (a) 4 wt% and (b) 10 wt% solutions of PEO in water.

drops during the breakup of the solution jet. It is likely that the secondary population observed in the distributions of the electrospun fibers is formed due to fiber splaying events, which were observed in our laboratory (Fig. 2b) and have been reported by other researchers [13–15,18]. At this time it is unclear whether the appearance of the bimodal size distribution only in fibers spun from higher concentration solutions is indicative of increased frequency of these events in more concentrated solutions or related to greater stability of small, secondary jets formed from higher concentration solutions, which have correspondingly lower surface tension (Fig. 8). Future work in our laboratory will include investigation of splaying events with high-speed photography to elucidate the mechanism of formation of the small fiber population.

3.3. Properties of electrospun textiles

The previous sections are primarily focused on how solution properties and electrostatic forces influence the formation and subsequent morphology of individual electrospun polymer fibers. In this section, we summarize some properties of the electrospun textiles, which may be relevant to their use in commercial applications. One property of the electrospun fiber textiles that is of interest is the total specific surface area associated with the textile. Electrospun fibers are recognized to possess high surface areas and large aspect ratios. There are numerous possible applications of electrospun textiles that take advantage of the large amount of surface area that is available in fabrics

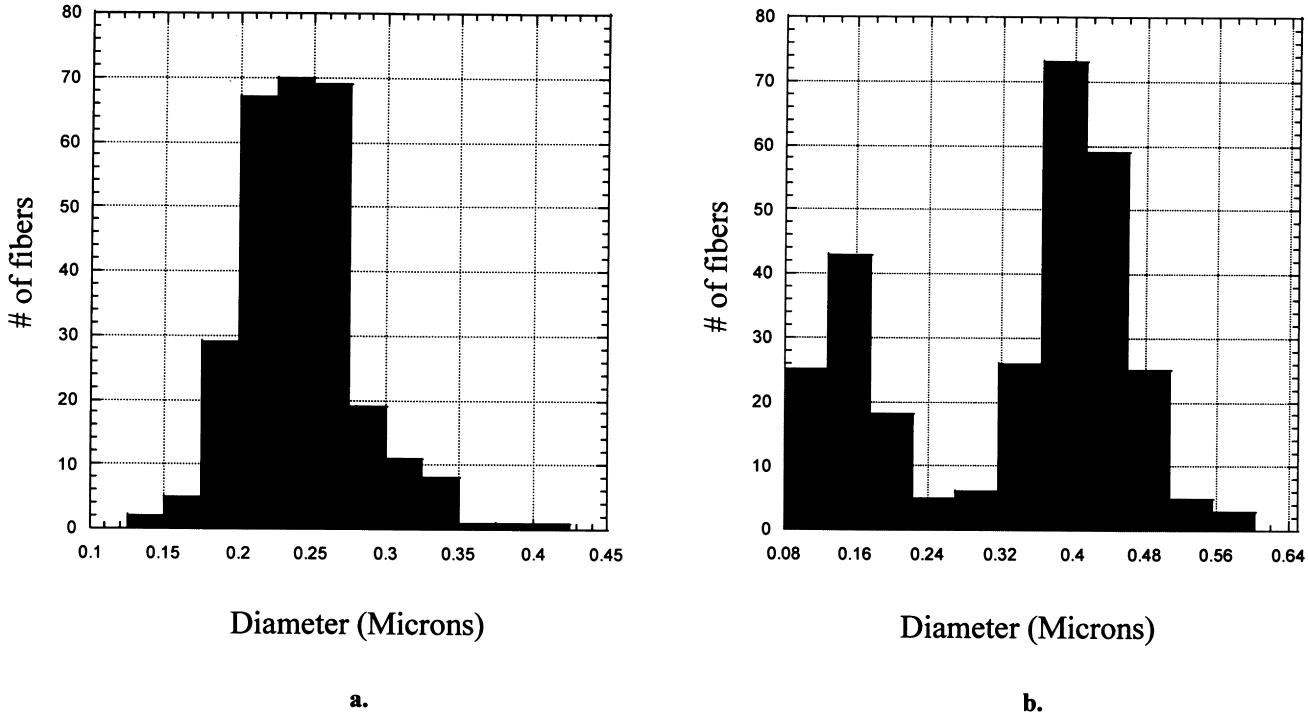

Fig. 10. Size distribution of diameters in nanofibers electrospun from PEO/water solutions: (a) 7 wt%; and (b) 10 wt%.

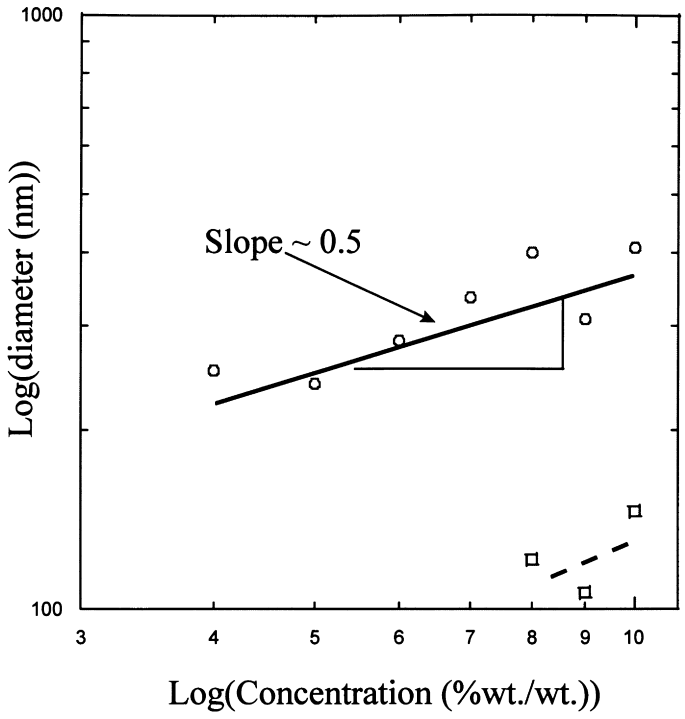

Fig. 11. Average fiber diameter as a function of PEO solution concentration. Primary distribution represented by circles, secondary distribution represented by squares.

composed of sub-micron fibers. The actual specific surface area of the electrospun textiles, obtained through Brunauer–Emmett–Teller (BET) measurements, ranged from 10 to 20 m^2/g (Fig. 13). These values are several orders of magnitude higher than what one would expect from fabrics composed of ordinary textile fibers, whose diameters are typically on the order of 10–100 μm. The BET measurements were not accurate enough to evaluate subtle changes

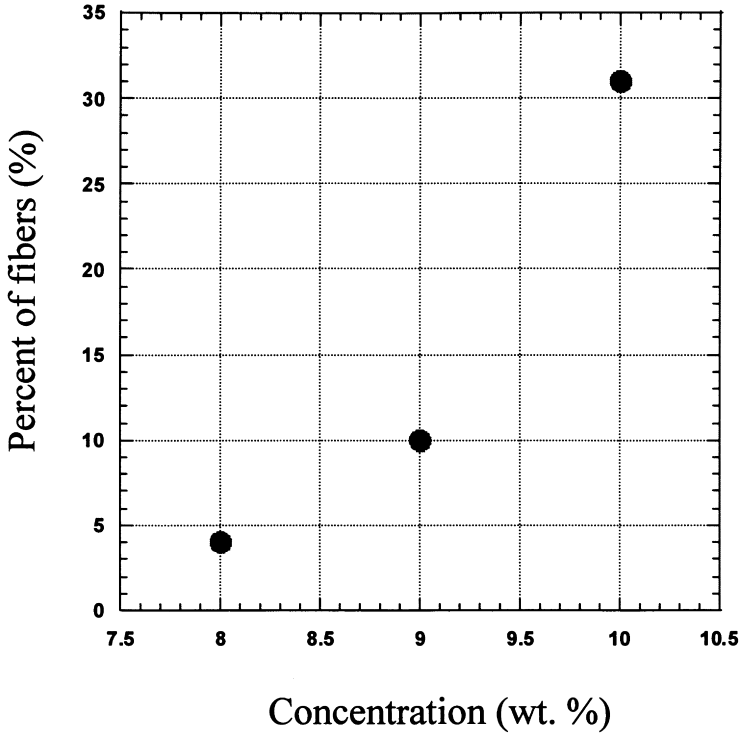

Fig. 12. Percentage of the number of electrospun fibers in the total population contributing to the secondary population, as a function of solution concentration.

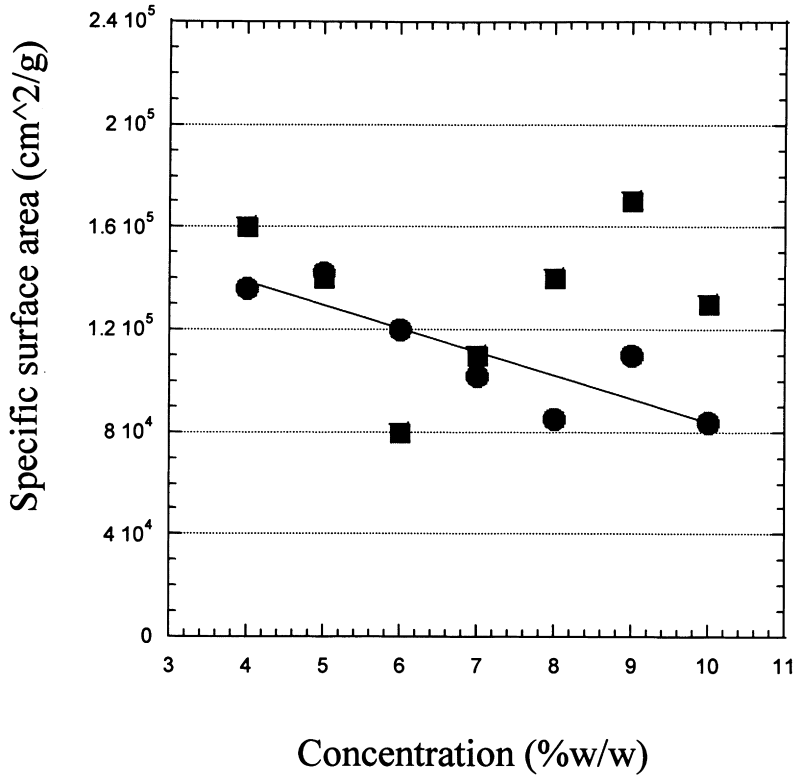

Fig. 13. Specific surface area in electrospun nanofiber textiles as a function of concentration of the spinning solution. Squares represent measured specific surface area, circles represent calculated specific surface area based on average fiber size measurements.

in specific surface area as a function of fiber size changes induced by changes in spinning solution concentration. However, the measurements may be used to check the accuracy of the fiber size measurements through comparison of the measured specific surface area and that calculated from the measured fiber diameters. The calculated and measured values of specific surface area are in reasonable agreement (Fig. 13), indicating that the average fiber diameter measurements presented here are representative of the whole electrospun textile.

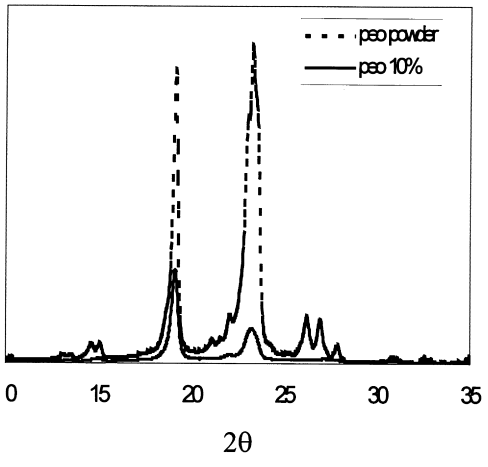

Fig. 14. WAXD patterns from PEO powder (dashed line) and PEO nanofibers electrospun from 10 wt% solution (solid line).

The crystalline properties of the electrospun fibers may also be of primary importance when considering the materials for commercial applications. To evaluate the structure, we have performed WAXD and DSC experiments on samples of PEO nanofiber textiles. Fig. 14 shows WAXD patterns for both a PEO nanofiber textile spun from a 10 wt% concentration PEO/water solution and the neat PEO powder from which the solution was made. The peak positions in each diffraction pattern are essentially identical, showing that there is no change in crystal structure induced by the electrospinning process. However, it is immediately evident that the diffraction peaks associated with the PEO powder are sharp and clearly defined while the peaks in the pattern from the non-woven textile are significantly broader, indicating that the crystalline order in the nanofibers was significantly less than in the powders. Similarly, the PEO nanofiber textiles had a melting temperature, T_m, and heat of fusion, ΔH_f, (66°C and 200 J/g, respectively) that were much lower than T_m and ΔH_f found for the neat powder (71°C and 250 J/g, respectively), indicating the overall crystallinity of the electrospun fibers was poor. These results are in qualitative agreement with the results presented by Buchko [5] and Larrondo [19–21] in which relatively low crystallinity was observed for polymer fibers electrospun from the melt state.

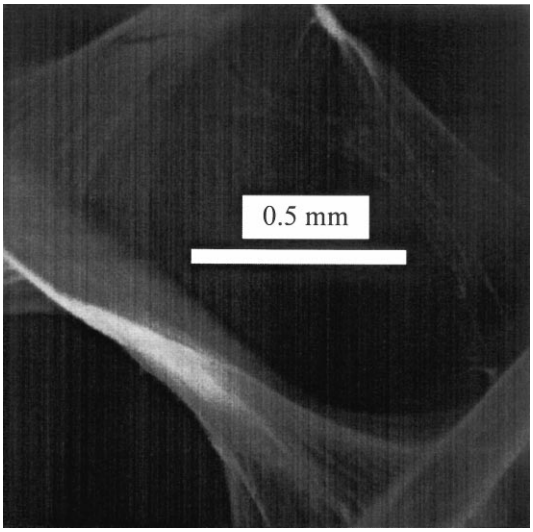

Fig. 15. Photomicrograph of a PEO webs electrospun from a 2 wt% solution onto an aluminum grid.

Finally, electrostatic effects have also been found to influence the configuration of electrospun textiles in ways that have potential for exploitation in the application of these materials. During the course of our research, a number of observations have been made, which suggest that under certain conditions the residual charge left on the electrospun fibers affect the way they will organize themselves in the non-woven textile. Specifically, the fibers will try and arrange themselves in such a way as to maximize contact with the electrically grounded target. For example, visual inspection of any electrospun textile that has been collected on a metal screen will reveal that it is thicker at points in contact with the wires.

Attempts to electrospin from solutions with low viscosities have resulted in the collection of electrospun fibers in geometries other than a two-dimensional fiber mat or film. An example of a 3D structure formed on electrospinning of PEO from dilute aqueous solution onto a wire screen is shown in Fig. 15. Instead of a uniform non-woven fiber textile, the material has collected preferentially on the wires ultimately building up a 3D cellular structure on the grid. Since these fibers are still wet when they reach the target, those fibers that try to span the distance between two-screen wires break, retracting into droplets on the wires, along with fibers that were deposited along a wire.

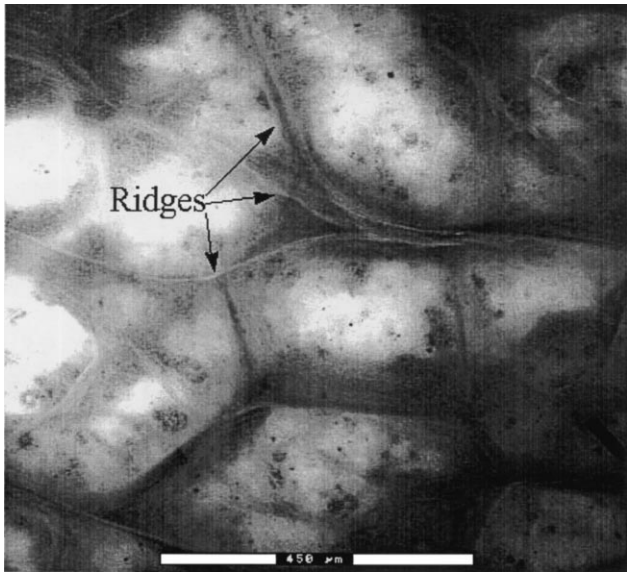

Fig. 16. 3D structure in a non-woven fiber mat electrospun from a 7 wt% solution of PEO in water electrospun at 11 kV onto a cloth substrate.

3D fiber structures have also been observed in fiber mats collected on other types of substrates. For example, a honeycomb structure that was electrospun at high voltage onto a piece of cloth backed by an aluminum screen is shown in Fig. 16. Because of the high electrospinning voltage, the spinning rate is faster and the electrospun fibers are arriving at the cloth substrate wet and full of bead defects, readily identifiable at high magnification (Fig. 17). These beads and fibers adhere to each other forming a thick, continuous layer of polymer particles that eventually builds up enough electrostatic charge to prevent new electrospun fibers from laying directly on the mat. Instead they are suspended slightly above the surface, where they have time to dry forming the 3D honeycomb structure we observe.

All the above examples show that the electrospun polymer that reaches an electrically grounded target can carry enough residual charge to influence the morphology of the textile formed. Though we found it possible to eliminate such structure by judicious choice of processing parameters, for certain applications the 3D networks of sub-micron fibers formed by electrostatic effects may be desirable.

4. Conclusions

In this work, the effects of processing parameters on the morphology of individual electrospun PEO nanofibers and the properties of electrospun non-woven fiber textiles has been explored. We have found that the morphology of the nanofibers produced is influenced strongly by parameters such as feed rate of the polymer solution, the electrospinning voltage, and the properties of the solution such as concentration, viscosity and surface tension. Increasing electrospinning voltage changed the shape of the surface from which the electrospinning jet originates. This shape change, which corresponds to a decrease in the stability of the initiating jet as the voltage is increased, has been correlated with an increase in the number of bead defects forming along the electrospun fibers. In addition, the onset of bead defect formation is shown to signal a change in the slope electrospinning current as a function of voltage. The properties of PEO solutions were found to define the processing window, and to influence the size and size distribution of nanofibers significantly.

The properties of solutions from which PEO fibers could be electrospun ranged from 4 to 10 wt% concentration and

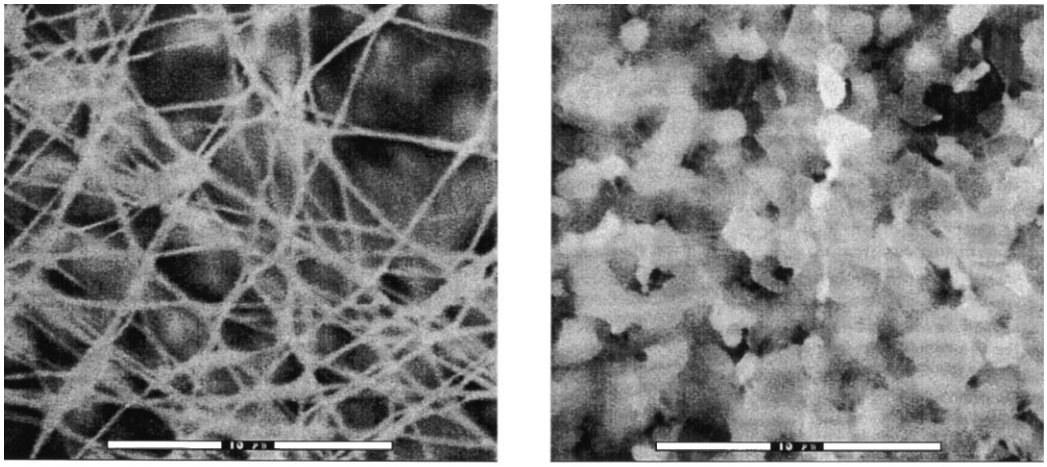

Fig. 17. High magnification images of the structure depicted in Fig. 16 at different working distances: (a) 9.84 mm working distance, focal plane on the surface of the ridge; and (b) 9.94 mm working distance, focal plane below the fibers on the surface.

had viscosities and surface tensions in the ranges of 1–20 poise and 55–35 dynes/cm, respectively. The diameter of the electrospun PEO fibers was found to increase with solution concentration according to a power law relationship. Fibers spun from solutions at concentrations of 8 wt% and higher, exhibited a bimodal distribution of diameters. Although this behavior has precedence in that bimodal size distributions have been observed for droplets formed by the similar process of electrospray, this is the first time that a bimodal distribution of sizes has been reported in a population of electrospun polymer fibers.

General properties of electrospun fiber textiles were also evaluated. The textiles were found to have specific surface areas in the rage of 10–20 m^2/g. Evaluation of structure by WAXD and DSC showed poor development of crystalline order in electrospun fiber mats. Finally, it has been demonstrated that under appropriate conditions, electrospun fibers may be made to organize into heterogeneous or 3D macroscale structures due to electrostatic effects, a property that has implications for commercial application of the technology.

Acknowledgements

The authors would like to thank Dr Darrell Reneker and his research group for their advice concerning all aspects of this work. In addition, we wish to thank Ibrahim Sendijarevic and Dr Anthony McHugh of the University of Illinois for providing viscosity measurements of polymer solutions, and Mr Joseph Rehrmann of the Soldier Chemical Biological Command-Edgewood Chemical and Biological Center for the BET measurements.

References

[1] Dees JR, Spruiell JE. Journal of Applied Polymer Science 1974;18:1053–78.
[2] Barham PJ, Keller A. Journal of Materials Science 1985;20:2281–302.
[3] Gibson PW, Shreuder-Gibson HL, Rivin D. AICHE Journal 1999;45:190–4.
[4] Gibson PW, Shreuder-Gibson H L. US Army Soldier and Biological Chemical Command Technical Report Natick/TR-99/016L 1999.
[5] Deitzel JM, Beck Tan NC, Kleinmeyer JD, Rehrmann J, Tevault D, Reneker D, Sendijarevic I, McHugh A. Army Research Laboratory Technical Report ARL-TR-1989, 1999.
[6] Buchko CJ, Chen LC, Shen Y, Martin DC. Polymer 1999;40:7397–407.
[7] Zeleny J. Physical Reviews 1914;3:69–91.
[8] Tayler GI. Proceedings of the Royal Society of London, Series A 1964;280:383–97.
[9] Tayler GI. Proceedings of the Royal Society of London, Series A 1969;313:453–75.
[10] Cloupeau M, Prunet-Foch B. Journal of Electrostatics 1990;25:165–84.
[11] Grace JM, Marijnissen JCM. Journal of Aerosol Science 1994;25:1005–19.
[12] Chen DR, Pui DYH, Kaufman SL. Journal of Aerosol Science 1995;26:963–77.
[13] Reneker DH, Chun I. Nanotechnology 1996;7:216–23.
[14] Srinivasen G, Reneker DH. Polymer International 1995;36:195–201.
[15] Doshi J, Reneker DH. Journal of Electrostatics 1995;35:151–60.
[16] Baumgarten PK. Journal of Colloid and Interface Science 1971;36:71.
[17] Fong H, Reneker DH, Chun I. Polymer 1999;40:4585–92.
[18] Reneker DH, Yarin AL, Fong H, Koombhongse S. Journal Applied Physics 2000;87:4531–47.
[19] Larrondo L, St. John Manley R. Journal of Polymer Science, Polymer Physics Edition 1981;19:909–20.
[20] Larrondo L, St. John Manley R. Journal of Polymer Science, Polymer Physics Edition 1981;19:921–32.
[21] Larrondo L, St. John Manley R. Journal of Polymer Science, Polymer Physics Edition 1981;19:933–40.
[22] Jaeger R, Bergschoof M, Martini I, Batlle C, Schonherr H, Vancso GJ. Macromolecular Symposium 1998;127:141–50.
[23] Fong H, Reneker DH. Journal of Polymer Science, Polymer Physics Edition 1999;37:3488–93.